Electronic Supplementary Material (ESI) for New Journal of Chemistry.

Rapid and Scalable Synthesis of Sulfur Quantum Dots through Ozone Etching: Photoluminescence and FRET mediated Co^{2+} Sensing

R V Reji,[a] V Biju*[a]

[a] Department of Physics, University of Kerala, Thiruvananthapuram- 695581, Kerala, India

Table S1. Comparison of different methods for the synthesis of luminescent SQDs from elemental sulfur.

Synthetic method	Reaction time (h)	Reaction temperature (°C)	PLQY (%)	Reference
Assembly-fission synthesis	125	70	3.8	1
Assembly-fission followed by H_2O_2 etching	125	70	23	2
Hydrothermal fission-aggregation mechanism	4	170	4.02	3
Oxygen acceleration	10	90	21.5	4
Ultrasonication-promoted synthesis	12	-	2.1	5
Copper-Ion-Assisted Precipitation Etching Method	74	70	32.8	6
Microwave-assisted synthesis	55	70	49.25	7
Bubbling-assisted strategy	96	70	8	8
Ultrasound-microwave-assisted etching with hydrogen peroxide	2	70	58.6	9
Solvothermal Synthesis	42	220	10.30	10
Dielectric barrier discharge-accelerated one-pot synthesis	20	-	2.0	11
Mechanical grinding assisted approach	1	-	21	12
Ethylenediamine-assisted solvothermal treatment	5	170	87.8	13
Ethylenediamine-assisted acceleration strategy	6	70	14.22	14
Ethanol assisted solvothermal treatment	36	220	7.04	15
solvent-type passivation strategy	4	160	8.7	16
Ozone assisted top- down approach	4	90	9.26	Present work

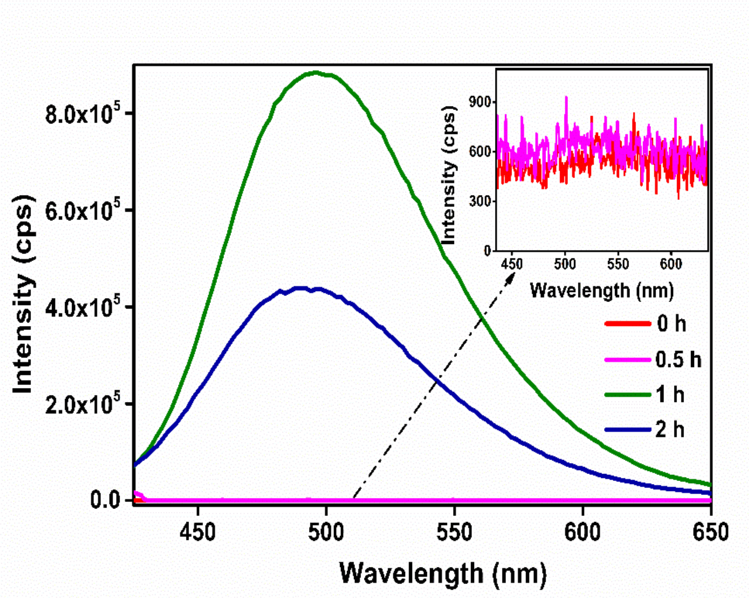

Fig. S1. PL spectra (excited at 410 nm) of S dots with different durations of ozone treatment as indicated on the frame.

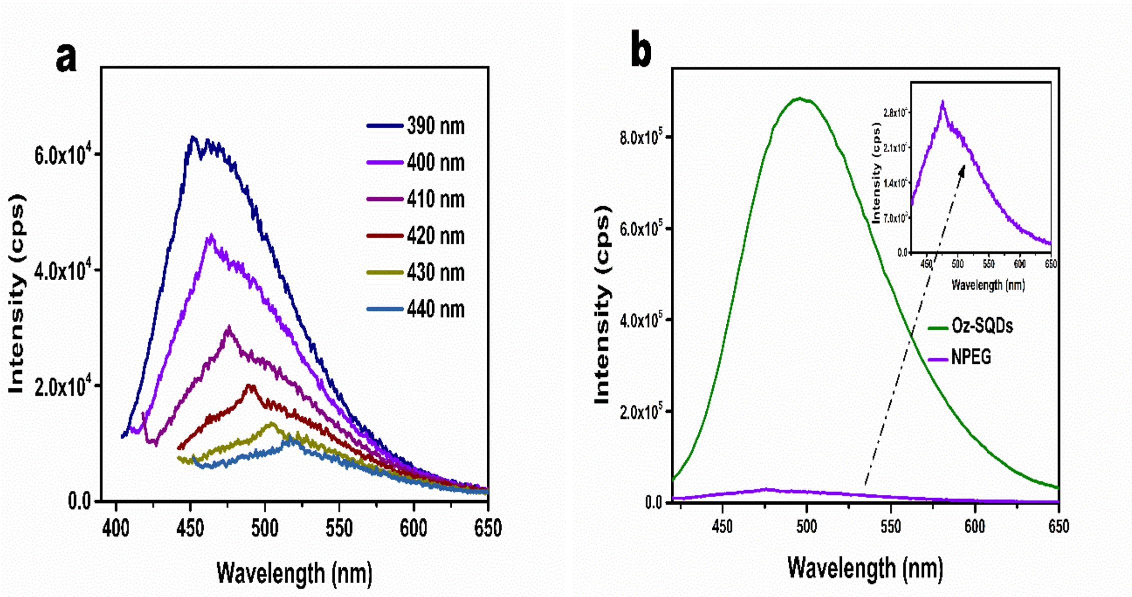

Fig. S2. (a) PL spectra of NPEG at different excitation wavelengths. (b) PL spectra (excited at 410 nm) of NPEG and Oz-SQDs.

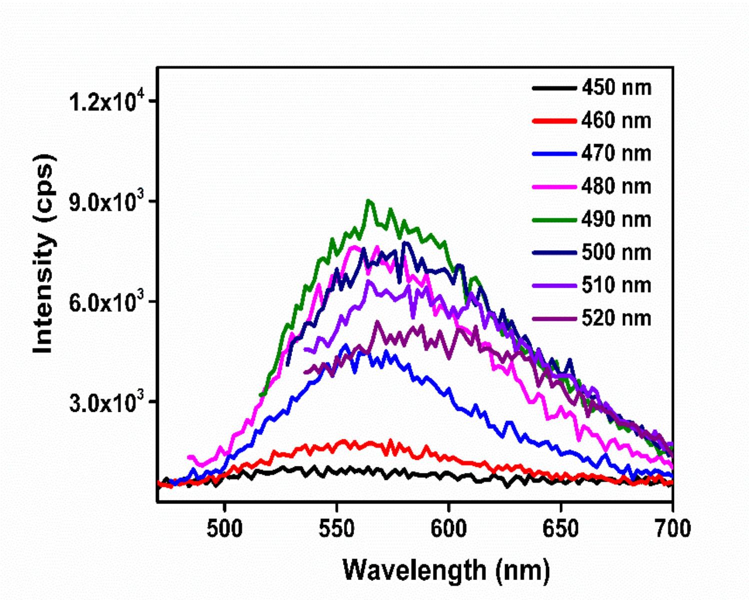

Fig. S3. Excitation-independent PL spectra of S dots.

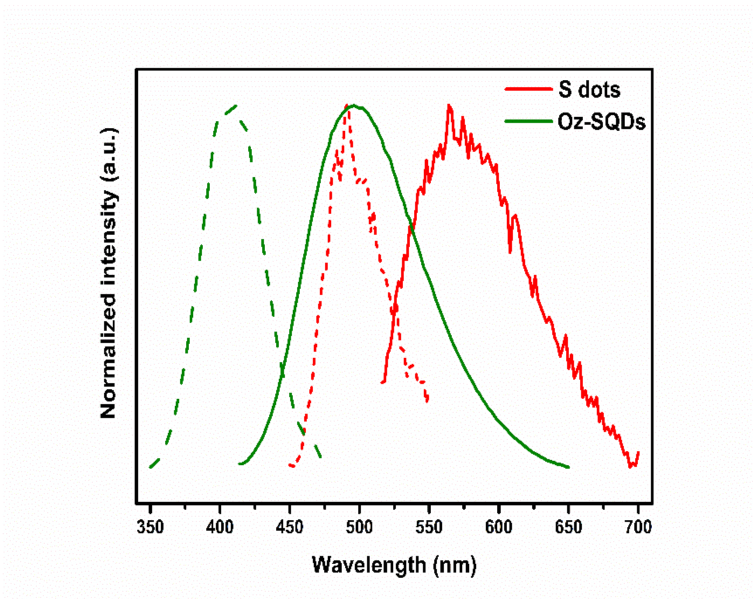

Fig. S4. PL (solid red line, excited at 490 nm), PLE (dash red line, detected at 575 nm) of S dots and PL (solid green line, excited at 410 nm), PLE (dash green line, detected at 496 nm) of Oz-SQDs.

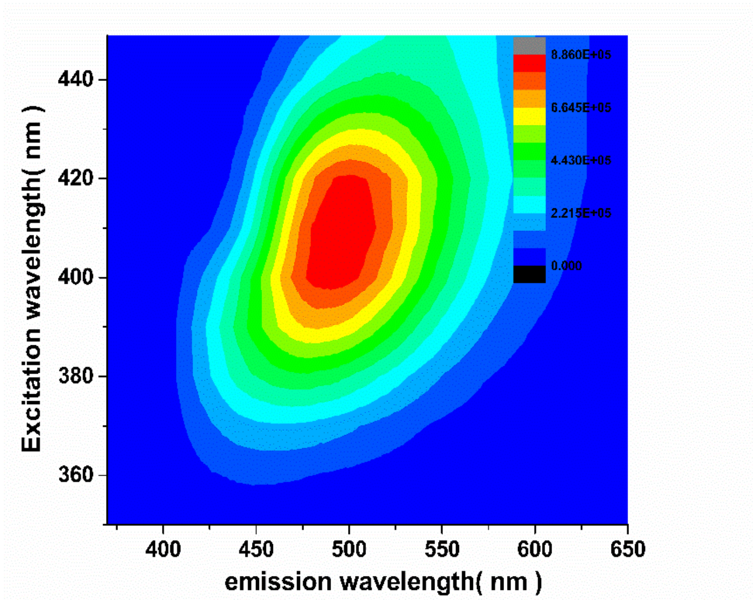

Fig. S5. The three-dimensional excitation and emission matrix (3D-EEM) fluorescence spectrum of Oz-SQDs.

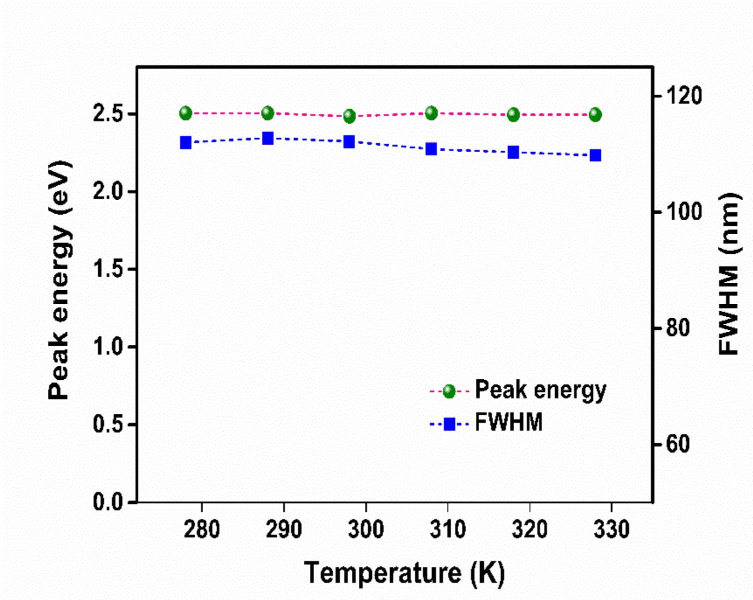

Fig. S6. PL peak energy and FWHM as a function of the temperature.

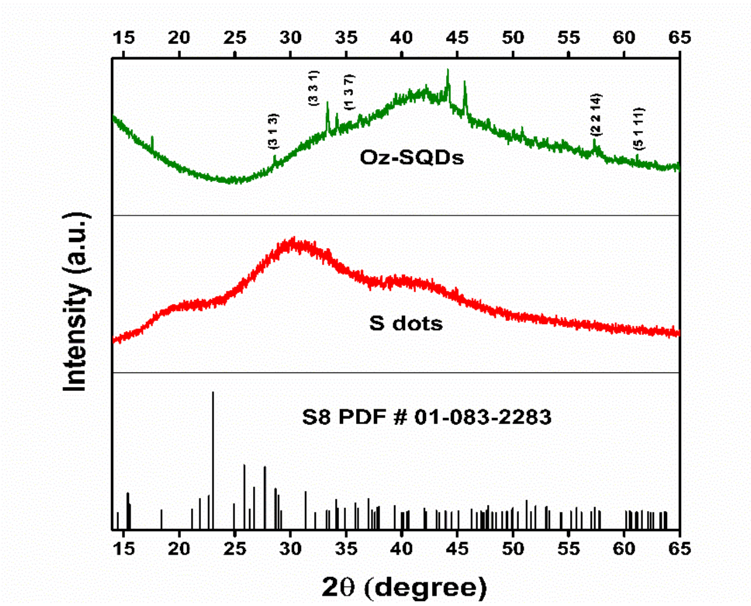

Fig. S7. XRD patterns of S dots and Oz- SQDs.

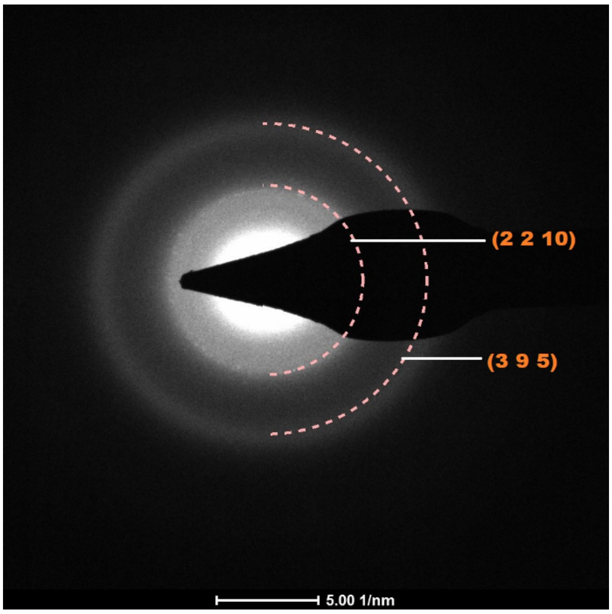

Fig. S8. SAED pattern of S dots.

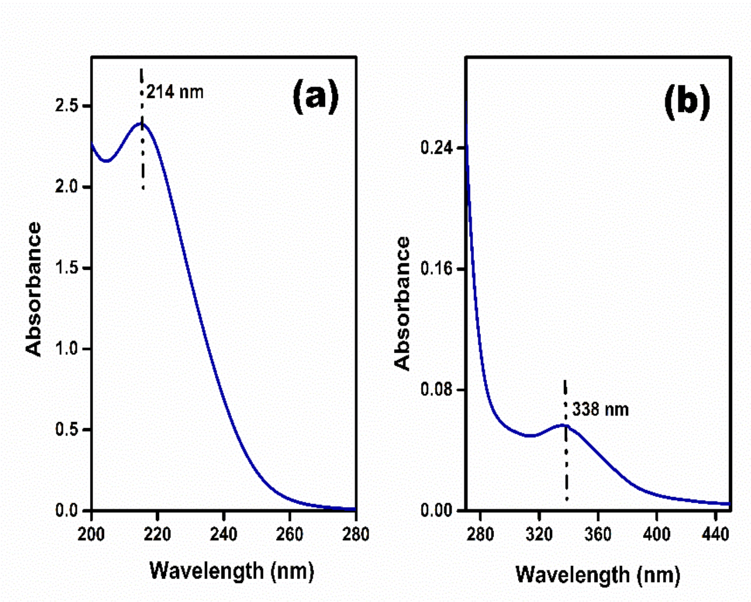

Fig. S9. UV-Visible absorption spectra of the sample with 2h ozone treatment after diluting (a) 2000 times with water (b) 100 times with water.

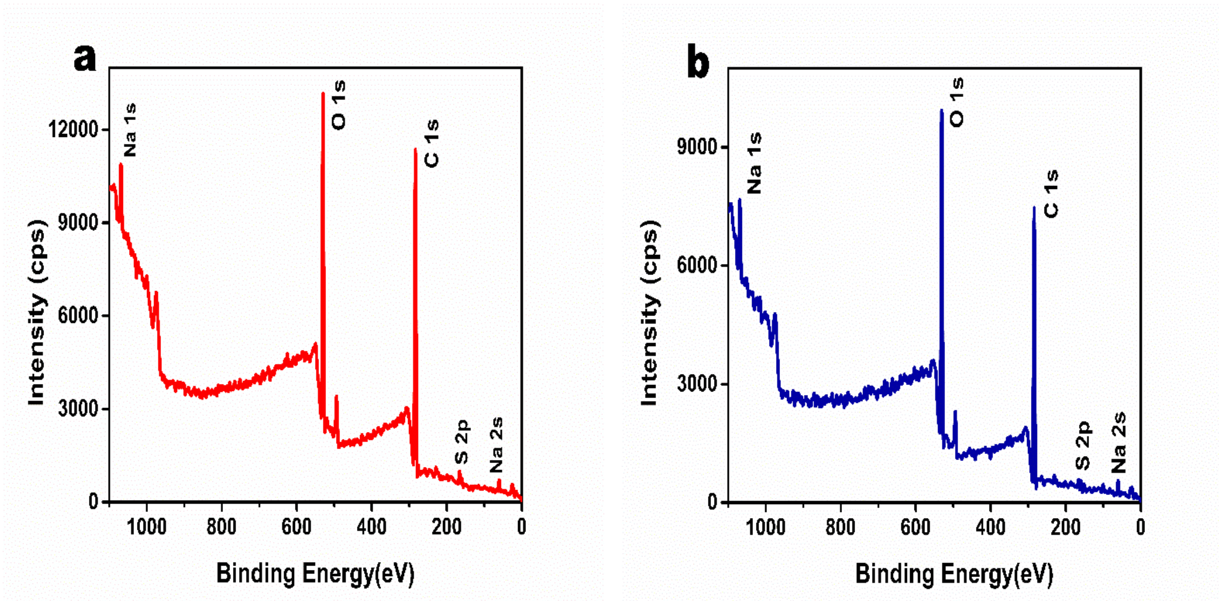

Fig. S10. (a) XPS survey spectra of (a) S dots (b) Sample with 2 h ozone treatment.

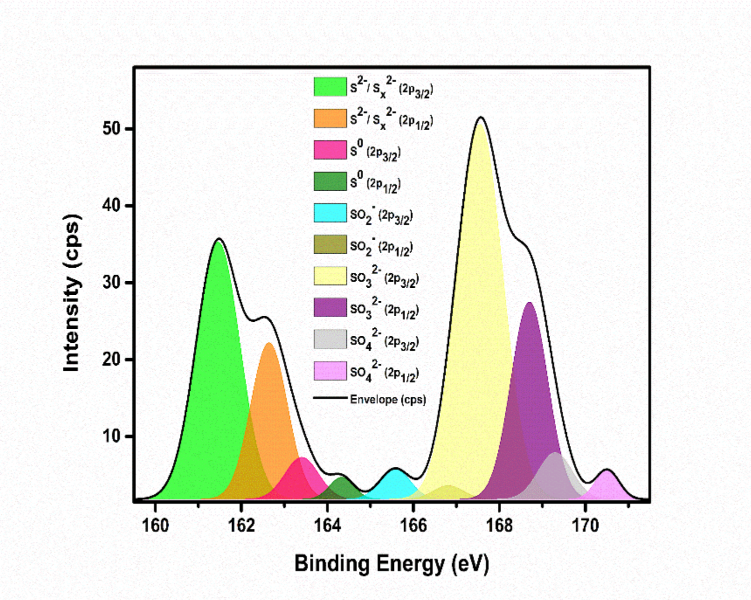

Fig. S11. S2p XPS spectrum of the sample with 2 h ozone treatment.

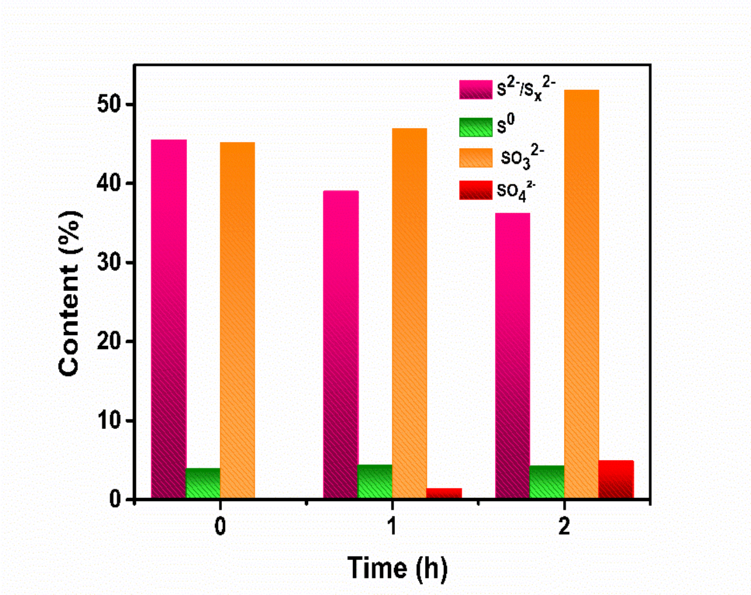

Fig. S12. Variation in the amount of different sulfur species with ozone treatment duration.

Table S2. Comparison of different methods for the determination of Co^{2+}.

Methods	Sensing material	Linear range (µM)	Detection limit (µM)	Reference
Fluorometric	Carbon dots	0 - 40	0.45	[17]
Fluorometric	Nitrogen and sulfur co-doped graphene quantum dots	0 - 40	1.25	[18]
Potentiometric	p-(4-n-butylphenylazo) calix[4]arene	9.2- 10000	4.00	[19]
Colorimetric	Biofunctionalized silver nanoparticles	5 - 100	7.00	[20]
Fluorometric	Sulfur quantum dots	0 - 90	0.02	[21]
Fluorometric	Sulfur quantum dots	0-25	1.57	[22]
Fluorometric	Cysteine-decorated sulfur dots	0 - 40	0.16	[23]
Fluorometric	Sulfur quantum dots	19.6 – 56.6	2.44	Present work

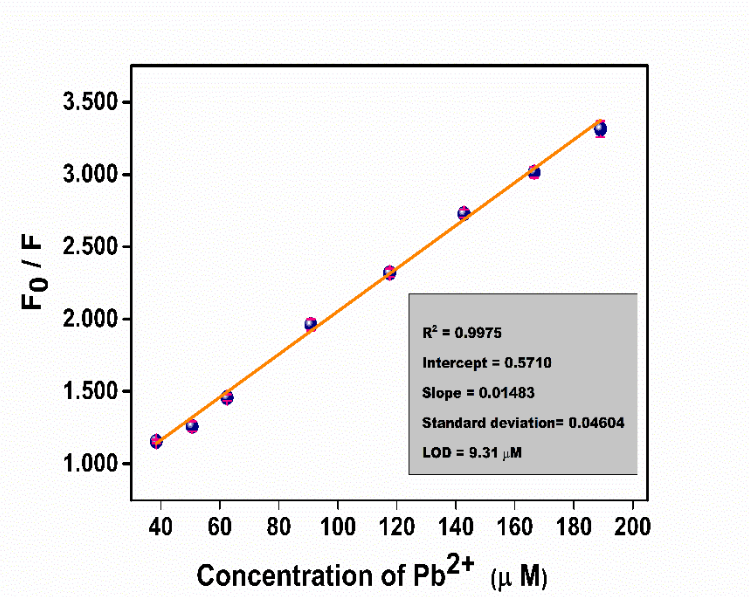

Fig. S13. F_0 /F value of the Oz-SQDs against different concentrations of Pb^{2+}.

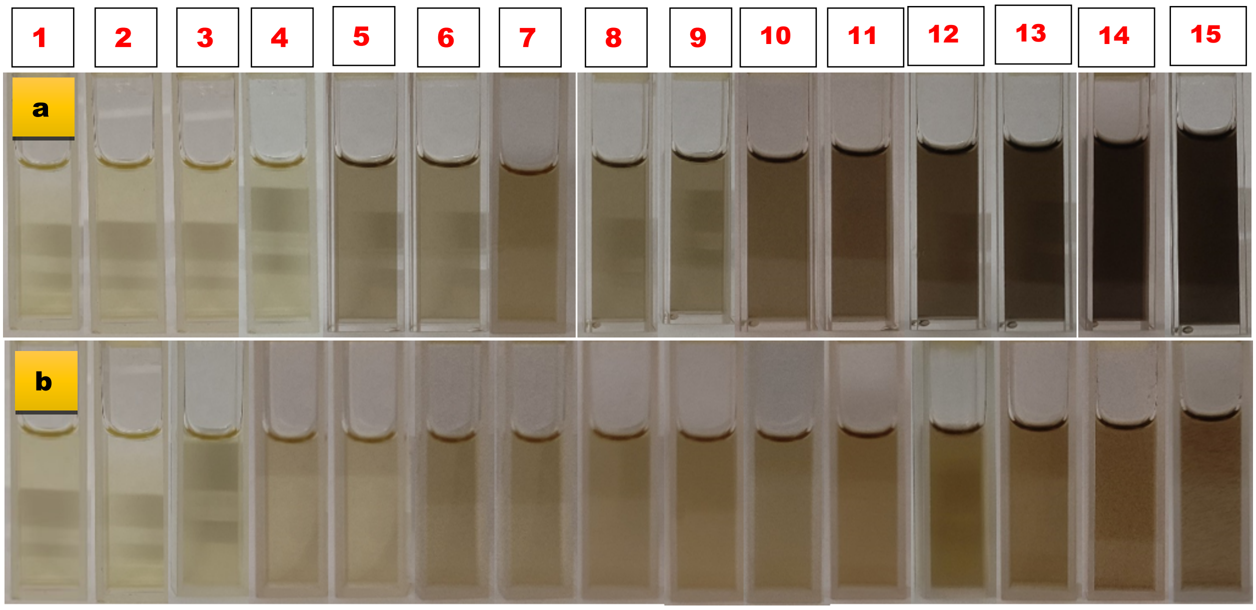

Fig. S14. Color of the Oz-SQDs aqueous solution after adding different concentrations of (a) Co^{2+} (b) Pb^{2+}

[(1). 0 µM, (2). 19.6 µM, (3). 22.8 µM, (4) 29.1 µM, (5) 32.2 µM, (6). 38.5 µM, (7). 44.6 µM (8) 56.6 µM, (9) 62.5 µM, (10). 90.9 µM, (11). 117.6 µM, (12). 142.8 µM, (13). 166.6 µM, (14). 210.5 µM, (15). 249.9 µM]

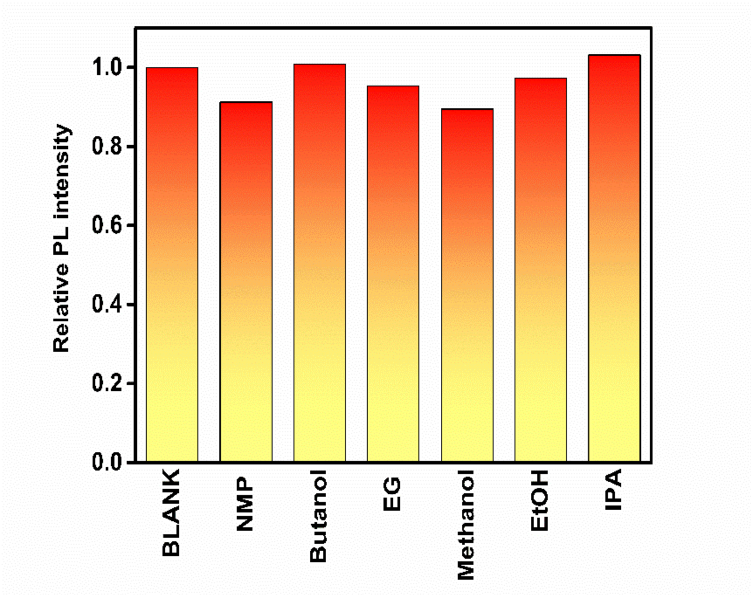

Fig. S15. Relative PL intensity of Oz-SQDs in the presence of different organic solvents (3 M); 1-Methyl-2-pyrrolidone (NMP), tert-Butanol (Butanol), Ethylene glycol (EG), Methanol, Ethanol (EtOH), Isopropyl alcohol (IPA).

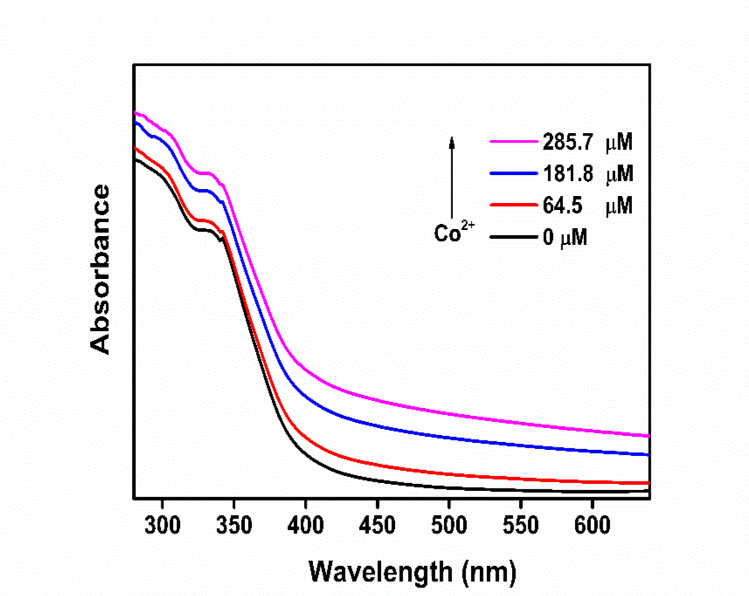

Fig. S16. UV-Visible absorption spectra of Oz-SQDs in the presence of different concentrations of Co^{2+}.

Table S3. PL lifetime components and corresponding amplitude fractions of Oz-SQDs and Oz-SQDs/ Co^{2+} system.

Sample	τ_1 (ns)	a_1 (%)	τ_2 (ns)	a_2 (%)	τ_{avg} (ns)
Oz-SQDs	**1.23**	**90.78**	**3.22**	**9.22**	**1.65**
Oz-SQDs/ Co^{2+}	**0.75**	**97.51**	**3.29**	**2.49**	**1.01**

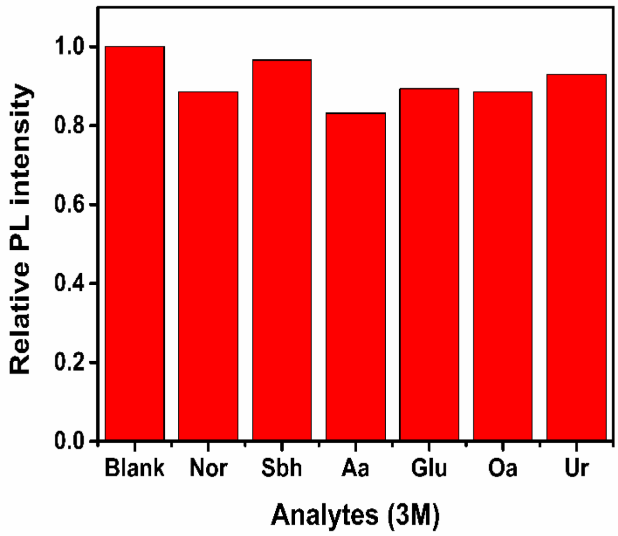

Fig. S17. Relative PL intensity of Oz-SQDs/ Co^{2+} system in the presence of various reducing agents; Norfloxacin (Nor), Sodium borohydride (Sbh), Ascorbic acid (Aa), Glucose (Glu), Oxalic acid (Oa) and Urea (Ur).

REFERENCES

1 L. Shen, H. Wang, S. Liu, Z. Bai, S. Zhang, X. Zhang and C. Zhang, *J. Am. Chem. Soc.*, 2018, **140**, 7878–7884.

2 H. Wang, Z. Wang, Y. Xiong, S. V. Kershaw, T. Li, Y. Wang, Y. Zhai and A. L. Rogach, *Angew. Chemie - Int. Ed.*, 2019, **58**, 7040–7044.

3 L. Xiao, Q. Du, Y. Huang, L. Wang, S. Cheng, Z. Wang, T. N. Wong, E. K. L. Yeow and H. Sun, *ACS Appl. Nano Mater.*, 2019, **2**, 6622–6628.

4 Y. Song, J. Tan, G. Wang, P. Gao, J. Lei and L. Zhou, *Chem. Sci.*, 2020, **11**, 772–777.

5 C. Zhang, P. Zhang, X. Ji, H. Wang, H. Kuang, W. Cao, M. Pan, Y. E. Shi and Z. Wang, *Chem. Commun.*, 2019, **55**, 13004–13007.

6 Q. Le Li, L. X. Shi, K. Du, Y. Qin, S. J. Qu, D. Q. Xia, Z. Zhou, Z. G. Huang and S. N. Ding, *ACS Omega*, 2020, **5**, 5407–5411.

7 Z. Hu, H. Dai, X. Wei, D. Su, C. Wei, Y. Chen, F. Xie, W. Zhang, R. Guo and S. Qu, *RSC Adv.*, 2020, **10**, 17266–17269.

8 S. Liu, H. Wang, A. Feng, J. Chang, C. Zhang, Y. Shi, Y. Zhai, V. Biju and Z. Wang, *Nanoscale Adv.*, 2021, **3**, 4271–4275.

9 Y. Sheng, Z. Huang, Q. Zhong, H. Deng, M. Lai, Y. Yang, W. Chen, X. Xia and H. Peng, *Nanoscale*, 2021, **13**, 2519–2526.

10 C. Wang, Z. Wei, C. Pan, Z. Pan, X. Wang, J. Liu, H. Wang, G. Huang, M. Wang and L. Mao, *Sensors Actuators, B Chem.*, 2021, **344**, 130326.

11 M. Yang, C. Li, Y. Tian, L. Wu, J. Hu and X. Hou, *Chem. Commun.*, 2022, **58**, 8614–8617.

12 K. S. Sunil, K. Bramhaiah, S. Mandal, S. Kar, N. S. John and S. Bhattacharyya, *Mater. Adv.*, 2022, **3**, 2037–2046.

13 P. Gao, Z. Huang, J. Tan, G. Lv and L. Zhou, *ACS Sustainable. Chem. Eng.*, 2022, **10**, 4634–4641.

14 F. Yan, M. Xu, J. Xu, Y. Wang, C. Yi, Y. Dong, X. Wang and J. Xu, *Sensors Actuators B Chem.*, 2022, **370**, 132393.

15 Z. Wei, W. Lu, C. Pan, J. Ni, H. Zhao, G. Huang and C. Wang, *Dalt. Trans.*, 2022, **51**, 10290–10297.

16 C. Wu, S. Zhang, Y. Zheng, A. Wang, Q. Zhao, W. Sun, W. Liu, C. Long and Q. Wang, *Inorg. Chem.*, 2022, **61**, 21157–21168.

17 D. Kong, F. Yan, Z. Han, J. Xu, X. Guo and L. Chen, *RSC Adv.*, 2016, **6**, 67481–67487.

18 W. Boonta, C. Talodthaisong, S. Sattayaporn, C. Chaicham, A. Chaicham, S. Sahasithiwat, L. Kangkaew and S. Kulchat, *Mater. Chem. Front.*, 2020, **4**, 507–516.

19 P. Kumar and Y. B. Shim, *Talanta*, 2009, **77**, 1057–1062.

20 Y. Yao, D. Tian and H. Li, *ACS Appl. Mater. Interfaces*, 2010, **2**, 684–690.

21 S. Wang, X. Bao, B. Gao and M. Li, *Dalt. Trans.*, 2019, **48**, 8288–8296.

22 F. Arshad and M. P. Sk, *ACS Appl. Nano Mater.*, 2020, **3**, 3044–3049.

23 L. Li, C. Yang, Y. Li, Y. Nie and X. Tian, *J. Mater. Sci.*, 2021, **56**, 4782–4796.